nature materials

Article

https://doi.org/10.1038/s41563-024-02046-0

Antithrombotic coating with sheltered positive charges prevents contact activation by controlling factor XII–biointerface binding

Received: 28 July 2023

Accepted: 8 October 2024

Published online: 12 November 2024

Check for updates

Haifeng Ji[1,2], Kai Yu[1,2], Srinivas Abbina[1,2], Lin Xu[3], Tao Xu[3], Shengjun Cheng[3], Sreeparna Vappala[1,2], S. M. Amin Arefi[4,5], Md Mohosin Rana[1,2], Irina Chafeeva[1,2], Matthew Drayton[1,2], Kevin Gonzalez[1,2], Yun Liu[6], Dana Grecov[4,5], Edward M. Conway[1,4,7], Weifeng Zhao[3] ✉, Changsheng Zhao[3] & Jayachandran N. Kizhakkedathu[1,2,4] ✉

Antithrombotic surfaces that prevent coagulation activation without interfering with haemostasis are required for blood-contacting devices. Such materials would restrain device-induced thrombogenesis and decrease the need for anticoagulant use, thereby reducing unwanted bleeding. Here, by optimizing the interactions with coagulation factor XII rather than preventing its surface adsorption, we develop a substrate-independent antithrombotic polymeric coating with sheltered positive charges. The antithrombic properties of the coating were demonstrated in vitro with human blood and in vivo using a carotid artery–jugular vein shunt model in rabbits. The coating exhibits a strong interaction with factor XII, but results in a low reciprocal activation of the contact pathway that triggers clot formation. These findings contradict the prevailing strategy of designing antithrombotic materials through protein-repelling surfaces. Overall, the polymeric coating we describe can benefit most blood-contacting devices and is a useful engineering guideline for designing surfaces with improved antithrombotic properties.

Blood is a complex tissue consisting of a multitude of proteins and cells, with a wide range of regulators to achieve a balanced state between anticoagulation and coagulation, thereby ensuring physiological flow in vivo. When synthetic surfaces are exposed to blood, the contact pathway of coagulation is activated, initially triggered via the cleavage of the zymogen factor XII (FXII) to its active form FXIIa[1–3]. Indeed, antithrombotic surfaces that can totally prevent the contact activation of coagulation are currently not available[4]. Thus, anticoagulants are often administered in conjunction with artificial devices or implants to prevent device/implant-associated thrombogenesis[5], but this inherently increases the bleeding risk[6,7]. A few different approaches have been investigated to prevent thrombus generation on surfaces with varying degrees of success, but they also have challenges[4,8–11].

Antithrombic surfaces can reduce thrombotic risk by preventing thrombogenesis without affecting haemostasis and is thus the holy grail of any blood-contacting surface design. Since the surface-induced conformational change in FXII is recognized as the first event that initiates coagulation activation[2,3,12], inhibiting FXII–surface interaction (for example, using antifouling surfaces) is intuitively a reasonable approach towards antithrombotic surfaces[13–16]. However, this strategy relies on the unproven premise that antifouling surfaces do not activate coagulation proteins that are desorbed from the surface. Although many surface designs based on protein repelling have claimed to possess the antithrombotic functionality[13–16], the close link between coagulation and anticoagulation in blood complicates these assertions. Furthermore, the dislodged clot or clot initiation at distant sites from

A full list of affiliations appears at the end of the paper. ✉e-mail: zhaoscukth@163.com; jay@pathology.ubc.ca

https://doi.org/10.1038/s41563-024-02046-0

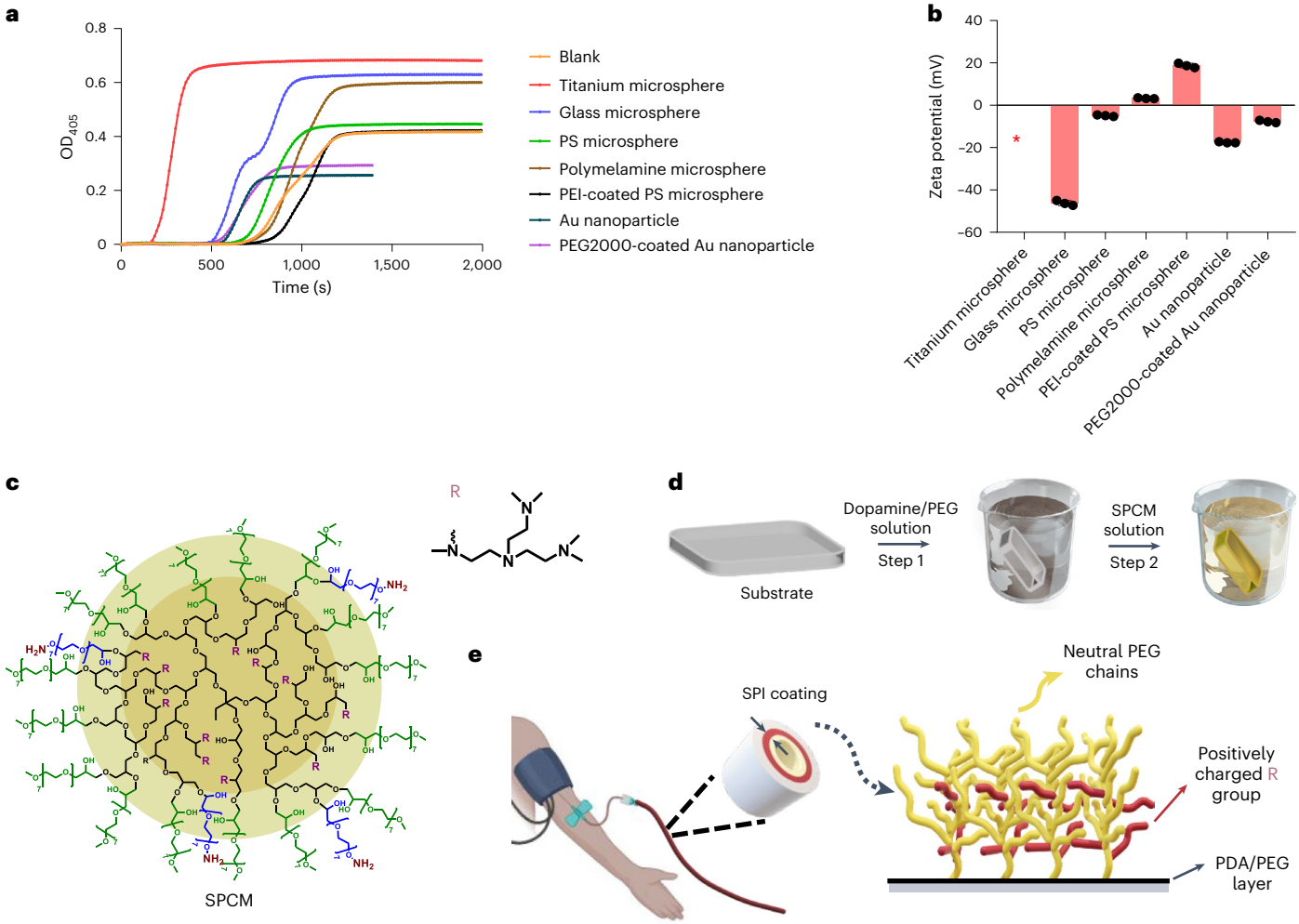

Fig. 1 | Concept and synthesis of SPI coating. a, Clotting time of recalcified plasma after incubation with different surfaces. OD_{405}, OD at 405 nm. At least $n = 3$ biologically independent measurements are used. PS, polystyrene. **b**, Zeta potential of different surfaces. The red asterisk indicates that the measurements cannot be performed for this particle. **c**, Chemical structure of SPCM. The molecule has an HPG core decorated with R-based cationic binding groups, and a brush layer of methoxy PEG (mPEG) to protect the R groups from non-specific interactions. The primary amine groups at the end of the PEG reacts with the quinone groups of the PDA/PEG coating to generate the SPI coating. **d**, Schematic of the generation of an SPI coating on different substrates. **e**, Cartoon illustrating the macrostructure and microstructure of an SPI-coated catheter used for the development of a blood-contacting device.

antifouling surfaces can lead to more serious consequences[17]. Besides, recent insights into the nature of loosely bound proteins have revealed that antifouling surfaces are unable to prevent the adsorption of many proteins in vivo[18–20] and thus have the potential to trigger coagulation.

Despite these uncertainties, the predominant and possibly the sole design approach for antithrombotic surfaces is based on inhibiting protein–surface interactions. Therefore, conducting a thorough analysis on their limitations and proposing a more promising strategy could serve as a crucial turning point in the design of true antithrombotic surfaces. Building on the current knowledge of blood-contacting surfaces, this study aims to (1) analyse why antifouling or protein/cell-repelling surfaces are not fully protected against thrombus formation; (2) to propose a new strategy for the design of a universal substrate-independent antithrombotic surface coating for blood-contacting applications; and (3) to demonstrate how the new surface coating can prevent surface-initiated thrombogenesis in vitro in human plasma, whole blood and in a relevant animal model.

Concept, design and synthesis of new antithrombotic coating

We began our studies by examining the effects of coagulation activation in the plasma of various surfaces with distinct surface properties. These included negatively charged surfaces (glass and titanium), positively charged surfaces (polymelamine and polyethylenimine (PEI)-coated polystyrene (PS)), hydrophobic surfaces (PS), metallic surfaces (titanium and gold) and neutral hydrophilic surfaces (polyethylene glycol (PEG)-modified gold) (Fig. 1a,b). Most of the tested synthetic surfaces were in their nanoparticulate form, including those with antifouling properties (PEG-modified gold), and they shortened the plasma-clotting time compared with plasma alone. The one exception to this finding, however, was positively charged surfaces, which had minimal effects on plasma clotting. This raised the possibility of a new approach to develop antithrombotic surfaces using cationic surfaces. However, conventional cationic surfaces are toxic in blood; such interfaces bind proteins, activate blood cells, initiate unwanted immune reactions and generate cell toxicity, possibly due to their strong electrostatic binding to proteins and cells[21,22]. Thus, we reasoned that developing a surface that does not initiate coagulation activation akin to cationic surfaces and simultaneously improve haemocompatibility could potentially lead to a new antithrombotic surface design. In our previous research, we have developed a library of biocompatible sheltered positively charged macromolecules (SPCMs) (for example, universal heparin reversal agents (UHRAs) and macromolecular polyanion inhibitors)[21,23–25]. Compared with naked

positively charged macromolecules, these SPCMs maintained strong interactions with target biomolecules while demonstrating favourable haemocompatibility.

Inspired by this, we designed a universal substrate-independent coating based on surface-conjugated SPCMs. We refer to this new surface as a selective protein interacting (SPI) coating to achieve control over the protein interaction and selective protein binding with sheltered positive charges. To develop the SPI coating, we initially synthesized an SPCM, which consists of a hyperbranched polyglycerol (HPG) core decorated with ~11 methylated tris(2-aminoethylamine) (R) groups and is protected with a shell layer of methoxy PEG (mPEG350) chains. The molecule is functionalized with approximately four primary amines at the end of PEG chains for surface conjugation (Fig. 1c). The synthesis scheme, characterization and properties of modified SPCM are shown in Supplementary Figs. 1–4.

The next step in the generation of the SPI coating is the development of a substrate-independent coating. A polydopamine (PDA)-based coating consisting of PDA/PEG covalently conjugated with SPCM was used, as this allows for its application to diverse biomedical devices or surfaces without pretreatment (Fig. 1d)[26]. The successful conjugation of SPCM on the PDA/PEG coating was verified by attenuated-total-reflectance Fourier transform infrared spectroscopy (Supplementary Fig. 5), X-ray photoelectron spectroscopy (Supplementary Fig. 6), quartz crystal microbalance (Supplementary Fig. 7) and ellipsometry (Supplementary Fig. 8). The stability of the SPI coating was confirmed by the absence of thickness change and spectral features by exposing the coating to harsh conditions (Supplementary Figs. 5, 7 and 8). The surface morphology of the SPI coating revealed a grainy uniform surface feature (Supplementary Figs. 9 and 10). The water contact angle of the SPI coating (~10°) confirms the highly hydrophilic nature of the coating (Supplementary Fig. 11a), and the surface zeta potential measurements (Supplementary Fig. 11b) showed that the SPI coating has a slight negative charge (−7 mV), unlike the SPCM or PDA/PEG coating. A more detailed surface characterization of the SPI coating is provided in the Supplementary Results. The proposed macrostructure of the SPI coating is shown in Fig. 1e.

SPI coating resists surface-induced thrombogenesis

Since most surfaces activate coagulation via the contact pathway, we investigated the effect of SPI coating on the contact pathway activation of blood coagulation in human plasma. The SPI coating was prepared on biomaterials with diverse surface chemistry that are commonly used for biomedical devices and implants. The cleavage efficiency of the chromogenic substrate S-2302 for FXIIa and kallikrein was used as a measure of contact activation after incubating the SPI-coated surfaces and control surfaces in plasma. As shown in Fig. 2a, contact activation by the SPI-coating-incubated plasma was significantly less compared with the uncoated surface, and showed no significant difference compared with the control plasma, whereas other hydrophilic control coatings such as PDA/PEG and HPG/PEG coatings maintain the surface-induced contact activation (Supplementary Fig. 12).

We next investigated whether the SPI coating induced the activation of other proteins in the contact pathway. Here we used glass as a positive control, which is a potent contact pathway activator. Compared with other coatings, the SPI coating significantly inhibited bradykinin (BK) generation (Fig. 2b) in plasma. The SPI coating also significantly inhibited thrombin generation as measured with the chromogenic substrate S-2238 (Fig. 2c), and the formation of thrombin–antithrombin (TAT) complexes (Fig. 2d)[27]. The SPI coating, furthermore, significantly prolonged the plasma-clotting time compared with other coated substrates (Fig. 2), as well as on coated polymeric catheters under shear conditions (60 s^{-1}) (Fig. 2f). These data provide the initial evidence of the antithrombotic properties of the SPI coating.

Additional clotting studies were performed in recalcified plasma using coated glass vials (Fig. 2g–j and Supplementary Video 1). An unmodified glass surface induced clot formation within 10 min (Fig. 2g), whereas the SPI coating prolonged the clotting time to more than 1 h (Fig. 2h). Furthermore, the SPI coating restrained clot formation on the surface without significantly interfering with the haemostatic function of plasma. This was shown by the following: after an initial 30 min incubation of plasma with the SPI coating, coagulation was triggered by introducing actin. Results show that clotting was not inhibited or delayed in plasma incubated with the SPI coating (Fig. 2i). Further, compared with traditional heparin coatings and antifouling surfaces, the SPI coating demonstrated superior antithrombotic functionality (Supplementary Figs. 13 and 14). Moreover, the antithrombotic functionality of the SPI coating remained robust even after prolonged storage, and its effectiveness was not significantly diminished even after the adsorption of other plasma proteins (Fig. 2j and Supplementary Figs. 15 and 16).

SPI coating is haemocompatible

Traditional anticoagulant materials/therapeutics can be complicated by disruptions in normal haemostasis, with a remaining risk of bleeding[12]. The SPI coating is not expected to interfere with normal coagulation; rather, it is designed to decrease surface-induced contact activation. As shown in Fig. 3a and Supplementary Fig. 17, prothrombin time (PT), activation partial thromboplastin time (aPTT), thrombin time (TT) and fibrinogen concentrations in plasma were not changed from normal after 30 min incubation with the SPI coating. The SPI coating also did not activate coagulation factor VII (FVII), thereby preventing the downstream activation of coagulation and fibrinolytic systems (Supplementary Fig. 18)[28]. A proteomic study was also used to confirm that the concentrations of different coagulation proteins in plasma incubated with the SPI coating did not appreciably change

Fig. 2 | SPI coating prevents surface-induced contact activation and thrombogenesis. a, Cleavage efficiency of the chromogenic FXIIa substrate S-2302 in human plasma incubated with different substrates with or without an SPI coating. **b**, BK generation in the plasma incubated with glass vials with and without coatings. Different coatings were compared. **c**, Cleavage efficiency of the chromogenic thrombin substrate S-2238 in recalcified plasma incubated with different coatings. **d**, TAT complex generation in recalcified plasma incubated with glass vials with and without coatings. **e**, Clotting time of the recalcified plasma incubated with glass or well plate with or without an SPI coating. **f**, Closed loop with silicone tubing with or without an SPI coating for the evaluation of the coating's antithrombotic function under shear condition. Left: the clotting time of the recalcified plasma incubated with a silicone catheter with or without an SPI coating. Right: photograph of the clot on the catheter at the end of the experiment. **g**–**j**, Photographs of the recalcified plasma incubated with a glass vial with or without an SPI coating after a predetermined procedure. Statistical analysis: for **a**, unpaired, two-tailed Student's *t*-test was applied for intragroup comparison for each substrate with or without an SPI coating. Two-way ANOVA with Bonferroni's post hoc analysis was applied for a comparison between the SPI-coated substrate and the negative control (PPP). For **b**–**d**, uncalcified PPP was used as the negative control. Multiple comparisons were performed using one-way ANOVA. If significance was determined, post hoc multiple comparisons analysis was conducted with a Tukey's test. For **e**, one-way ANOVA was applied for intragroup comparison for each substrate with different coatings. If significance was determined, post hoc multiple comparisons analysis was conducted with a Tukey's test. For **f**, unpaired, one-tailed Student's *t*-test was applied. If not specified otherwise, $n = 3$ biologically independent analyses were performed. All values are expressed as the mean ± s.d. If not specified otherwise, individual *P* values represent comparisons with the negative control. Exact *P* values are provided in the corresponding figures. Statistical significance was defined as $P < 0.05$.

https://doi.org/10.1038/s41563-024-02046-0

from normal (Fig. 3b and Supplementary Table 1), especially for those proteins involved in the contact activation (Fig. 3c).

Activated FXII can trigger the downstream activation of coagulation. To explore the potential impact of SPI coating on the coagulation system in the absence of an anticoagulant, we incubated recalcified plasma with glass and SPI-coated glass and stopped the coagulation reaction at designed intervals by re-adding sodium citrate. The PT, aPTT and TT values were markedly prolonged when plasma was incubated with a bare glass surface (Fig. 3d) due to the depletion of coagulation factors, particularly fibrinogen. In comparison, the SPI coating did not affect the PT or TT value, whereas the aPTT value was slightly prolonged. The prolonged aPTT observed in SPI-coating-incubated plasma may be attributed to the inevitable contact activation of air exposure in our experimental conditions. The activated coagulation factors that are promptly neutralized by other inhibitory proteins, such as C1 esterase inhibitor (C1INH) and antithrombin, resulting in

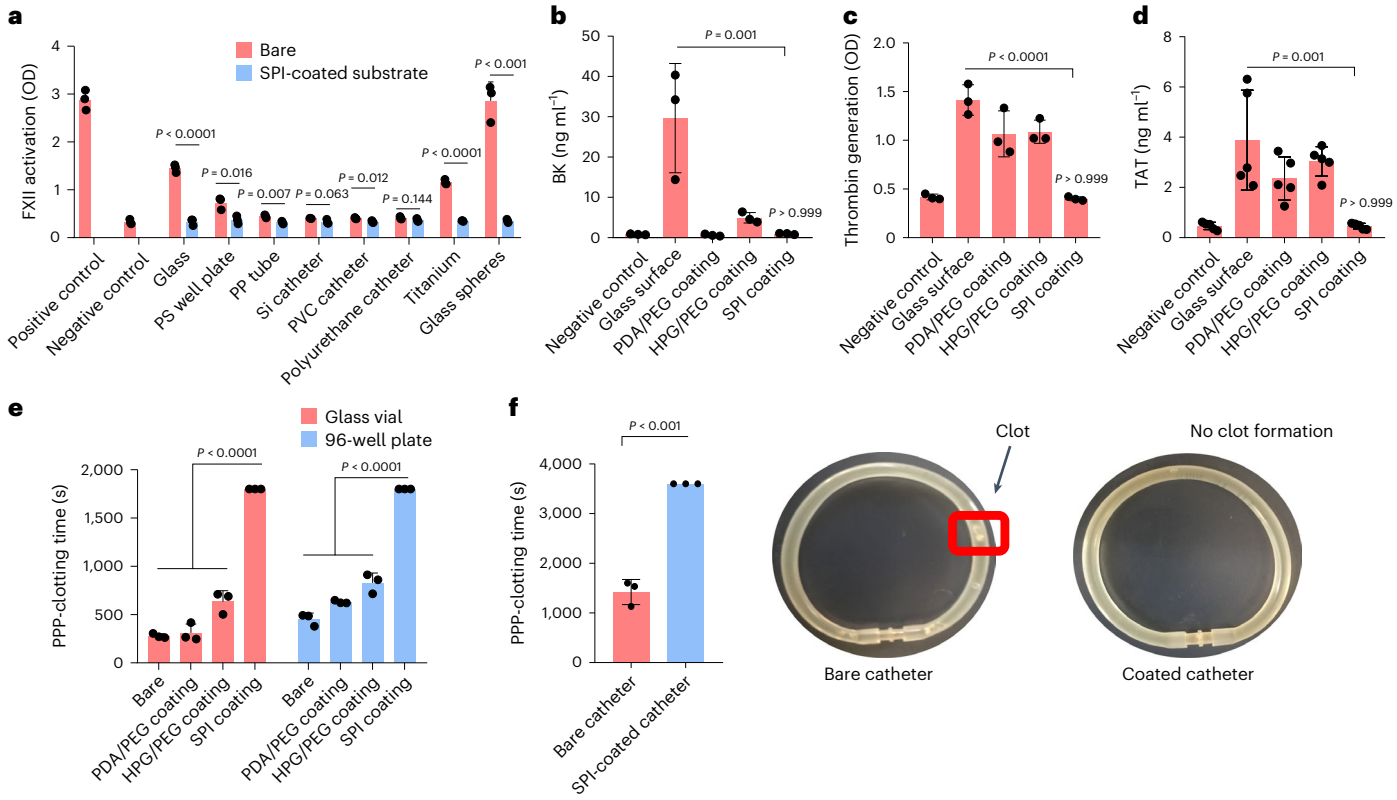

https://doi.org/10.1038/s41563-024-02046-0

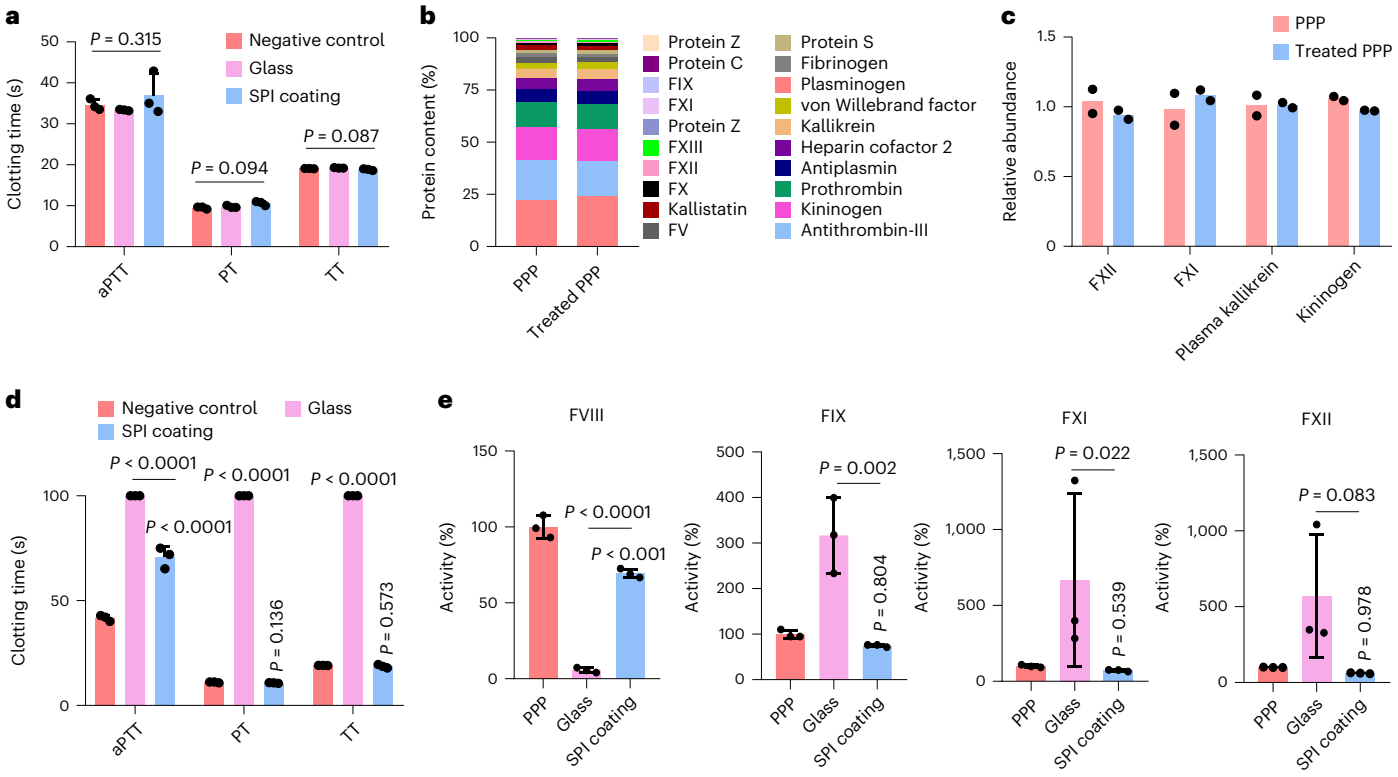

Fig. 3 | SPI coating prevents thrombin generation without interfering haemostasis. a, TT, aPTT and PT were measured using human PPP after incubation with bare and SPI-coated glass vials (PPP was used as the negative control; $n = 3$ biologically independent samples; all values are expressed as the mean ± s.d.). One-way ANOVA was used for intragroup comparison and no significant difference was found. **b**, Abundance of coagulation proteins as the percentage of total proteins in the plasma pre- and post-incubation with SPI coating ($n = 2$ biologically independent samples; all values are expressed as the mean). **c**, Relative abundance of contact-system-related proteins in the plasma pre- and post-incubation with an SPI coating ($n = 2$ biologically independent samples). **d**, TT, aPTT and PT in recalcified PPP after incubation with bare and SPI-coated glass vial (PPP was used as the negative control; $n = 3$ biologically independent samples; all values are expressed as the mean ± s.d.). One-way ANOVA was used for intragroup comparison for each substrate with different coatings. If significance was determined, post hoc multiple comparisons analysis was conducted with a Tukey's test. **e**, Activity of FVIII, FIX, FXI and FXII belonging to the intrinsic pathway of the plasma after incubation with bare and SPI-coated glass vial ($n = 3$ biologically independent samples; all values are expressed as the mean ± s.d.). One-way ANOVA was used for intragroup comparison for each substrate with different coatings. If significance was determined, post hoc multiple comparisons analysis was conducted with a Tukey's test. If not specified otherwise, individual P values represent comparisons with the PPP control. Exact P values are provided in the corresponding figures; statistical significance was defined as $P < 0.05$.

the depletion of intrinsic coagulation factors, which, in turn, causes the slight prolongation of aPTT[29]. Further analysis revealed that the activities of factor IX (FIX), factor XI (FXI) and FXII were significantly boosted, whereas that of factor VIII (FVIII) was depleted from the plasma on glass incubation. However, the activities of FIX, FXI and FXII were only slightly attenuated in SPI-coating-incubated plasma (Fig. 3e). The SPI coating also resists the adhesion and activation of platelets and neutrophils (Supplementary Figs. 19–25) as well as shows good cell compatibility (Supplementary Figs. 26–28) and low complement activation (Supplementary Figs. 29 and 30). Details are analysed and given in the Supplementary Results.

SPI coating is antithrombotic in an arteriovenous shunt model

We investigated the antithrombotic function of the SPI coating using an arteriovenous (AV) shunt model in rabbits to evaluate intracatheter thrombosis without anticoagulant administration[16,30]. The experimental design is shown in Fig. 4a. Blood flow is from the carotid artery to the jugular vein through an indwelling needle connected to a polyvinyl chloride (PVC) catheter, which is either modified with an SPI coating or used without modification. The experiments were performed for 30 min. To assess the haematological parameters of the animals during the procedure, blood samples were collected before and after the experiment. The coagulation function of the animals remained normal throughout the experiment as measured by the aPTT, PT and TT (Fig. 4b). There were also no significant changes in the body temperature (Supplementary Table 2), whole blood cell count (Supplementary Fig. 30) and other parameters (Supplementary Table 3) during the procedure.

Thrombus formation within the catheter was measured (Fig. 4c,d). After 30 min, the uncoated catheter induced severe intracatheter thrombosis (Fig. 4c) and blood flow through the catheter was almost stopped (Fig. 4d) and the catheter was blocked (Fig. 4e). However, the SPI-coated catheter significantly reduced surface-induced thrombosis (Fig. 4c). No significant difference was observed in the blood flow rate through the SPI-coated catheter at 30 min compared with the flow rate at the start of the experiment (Fig. 4d). The data showed that the SPI-coated catheter maintained patency (Fig. 4e). Moreover, the clotting time of the blood collected from the bare catheter after the procedure was significantly shortened compared with blood collected at the start of the experiment. There was no significant difference in clotting time between the blood collected from the SPI-coated catheter before and after the procedure (Fig. 4f). The data indicated that coagulation was activated on the uncoated catheter surface and the SPI-coated catheter resisted activation. Moreover, thrombus adherence to the SPI-coated catheters was significantly reduced (Fig. 4h) compared with the unmodified catheters (Fig. 4g), as shown in the digital and scanning electron microscopy images. However, we observed some clot deposition on part of the SPI-coated catheter connected to the

https://doi.org/10.1038/s41563-024-02046-0

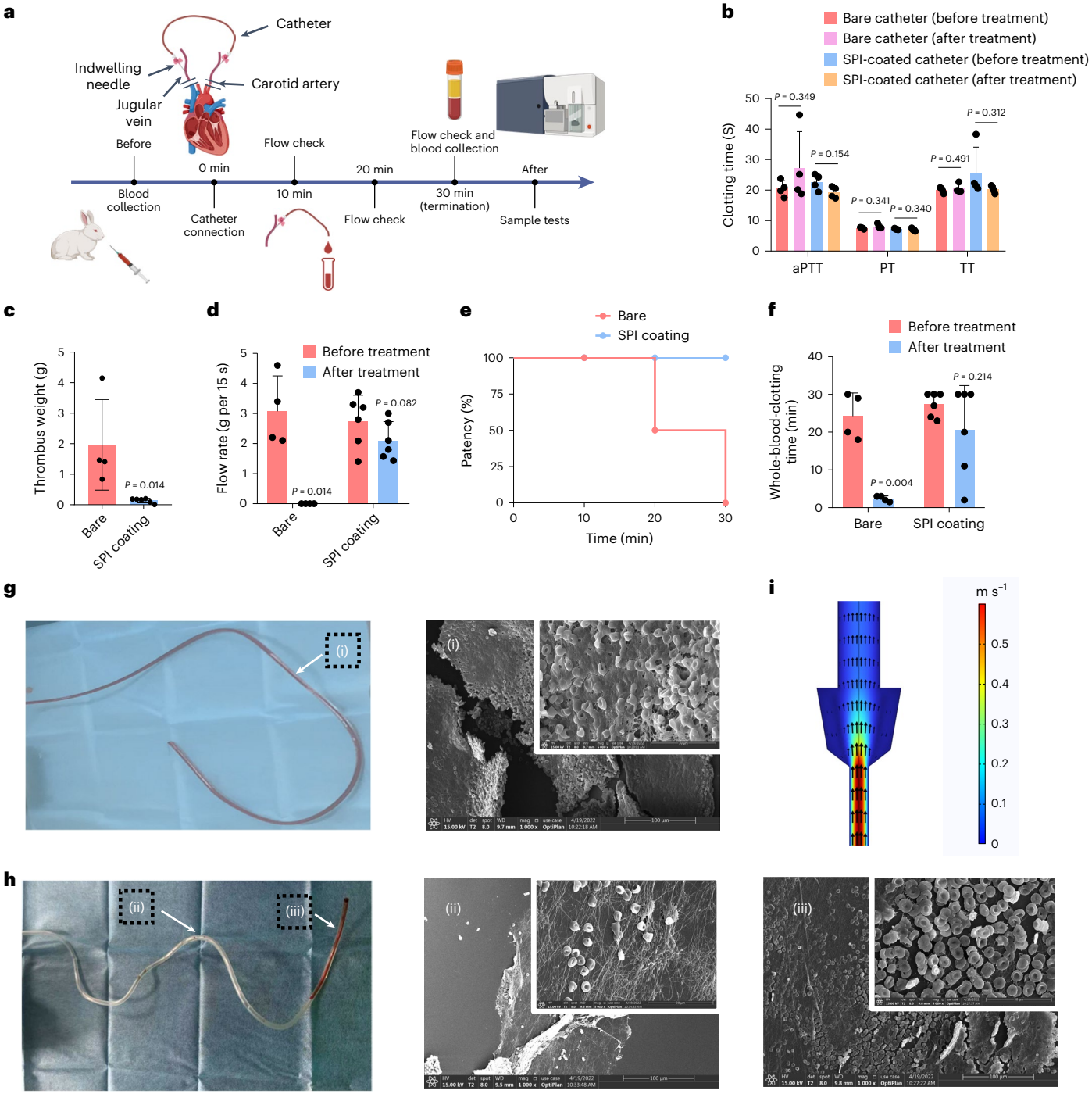

Fig. 4 | SPI coating is antithrombotic in the AV shunt model. a, Schematic showing the experimental setup to evaluate the antithrombotic characteristics of the SPI coating in an AV shunt model in rabbits without anticoagulant administration. **b**, Comparison of aPTT, PT and TT for the bare or SPI-coated catheter before and after treatment in rabbits. Paired one-way ANOVA was applied for intragroup comparison and no significant difference was found. **c**, Comparison of thrombus weight for the bare (uncoated) or SPI-coated catheter after treatment. Unpaired, two-tailed Student's *t*-test was applied. **d**, Comparison of blood flow rate through the uncoated or SPI-coated catheter before and after treatment. Paired, two-tailed Student's *t*-test was applied for intragroup comparison. **e**, Comparison of the flow patency of the blood through the uncoated or SPI-coated catheter at different time intervals. **f**, Clotting time of the whole blood collected from the uncoated or SPI-coated catheter before and after treatment. Paired, two-tailed Student's *t*-test was applied for intragroup comparison. **g**,**h**, Digital (left) and scanning electron microscopy (right) photographs for the blood clotting adhered on the uncoated catheter (**g**) and SPI-coated catheter (**h**). **i**, Computational fluid dynamics model for the catheter-indwelling needle connection. $n = 4$ biologically independent samples for the uncoated catheter group and $n = 6$ biologically independent samples for the SPI-coated catheter group. All values are expressed as the mean ± s.d. Exact *P* values are provided in the corresponding figures; statistical significance was defined as $P < 0.05$.

artery through the narrow needle (Fig. 4h(iii)). We attribute this to the dramatic change in local haemodynamics (Fig. 4i and Supplementary Fig. 31) when blood flows through the narrow needle and exits into the catheter, as simulated by computational fluid dynamics. The alternation in haemodynamics results in platelet activation, leading to local coagulation activation[31,32]. Since the SPI coating does not have inherent anticoagulant properties, it is unable to prevent clotting activation arising from non-self-induced factors.

https://doi.org/10.1038/s41563-024-02046-0

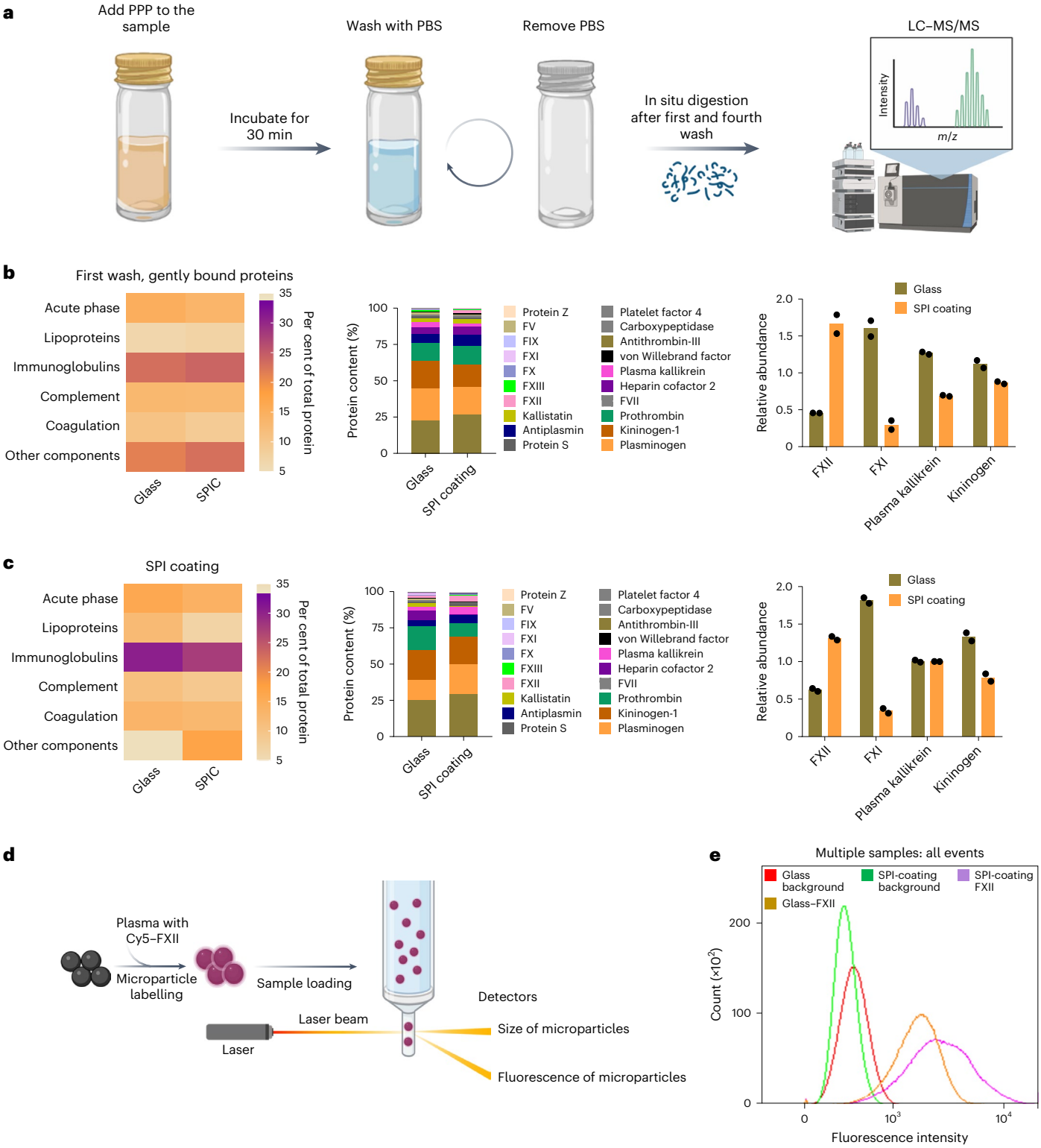

SPI coating strongly interacts with FXII without activation

Although we showed that the SPI coating significantly reduced contact activation and thrombogenesis, it is not clear as to how the SPI coating generates this activity. We analysed the adsorbed protein corona on the SPI coating from plasma to understand the role of biointerface-adsorbed proteins and their antithrombotic functions. The adsorbed proteins can be loosely or tightly bound to the surface, and their composition and surface organization can potentially affect the functionality of the material surface (Supplementary Figs. 32–34)[33,34]. Thus, we designed different washing steps to investigate the composition of loosely and tightly bound proteins by proteomics analysis, respectively, on glass and SPI-coated surfaces (Fig. 5a)[19].

After gentle washing, the loosely bound proteins were largely retained on both surfaces. Although the amounts of proteins were similar, the bare glass and SPI-coated surfaces showed different compositions (Fig. 5b, Supplementary Fig. 35a and Supplementary Table 4). The glass surface adsorbed more coagulation proteins and lower amounts

Fig. 5 | FXII strongly binds to an SPI-coated surface. a, Schematic for the detection of loosely or tightly bound proteins on bare or SPI-coated glass surface by proteomic analysis. **b**, Composition of loosely bound proteins on bare or SPI-coated glass surface by proteomic analysis. Left: abundance of each functional protein group as the percentage of total proteins. Middle: abundance of coagulation proteins as the percentage of total proteins. Right: comparison of the relative abundance of contact-system-related proteins loosely adsorbed on bare or SPI-modified glass surface. $n = 2$ biologically independent samples; all the values are expressed as the mean. **c**, Composition of tightly bound proteins on bare or SPI-modified glass surface by proteomic analysis. Left: abundance of each functional protein group as the percentage of total proteins. Middle: abundance of coagulation proteins as the percentage of total proteins. Right: a comparison of the relative abundance of contact-system-related proteins tightly adsorbed on bare or SPI-coated glass surface. $n = 2$ biologically independent samples; all values are expressed as the mean. **d**, Schematic of the in situ FXII adsorption behaviour on the surface. Glass microspheres with or without an SPI coating were incubated with FXII-deficient plasma externally added with Cy5-labelled FXII. The fluorescence intensity of the Cy5-labelled FXII adsorbed onto the surface was in situ detected by the flow cytometry method. **e**, Fluorescence intensity of the surfaces before and after Cy5-labelled FXII adsorption. Since the entire process does not involve surface separation and washing, the adsorbed proteins are retained as much as possible. The content of FXII in both hard protein corona and soft protein corona on the surface is reflected by the fluorescence intensity. The higher the fluorescence intensity, the more Cy5-labelled FXII is incorporated onto the material surface (500,000 events were recorded for each sample in FXII-deficient plasma). $n = 3$ biologically independent samples. The fluorescence intensity on the surface was measured after 30 min incubation. LC–MS/MS, liquid chromatography tandem mass spectrometry.

of immunoglobulins than the SPI coating. We then focused on proteins in the contact activation system, and found that the SPI-coated surface adsorbed more FXII than on the glass surface. The amounts of FXI, prekallikrein and kininogen on the SPI-coated surface were lower than those on the glass surface. Thorough washings distinguished the compositions of loosely bound and tightly bound proteins[33]. The glass surface adsorbed more immunoglobulins and coagulation proteins than the SPI coating. However, the SPI-coated surface had more adsorbed FXII than the glass surface (Fig. 5c, Supplementary Fig. 35b and Supplementary Table 5). The data illustrated that the SPI-coated surface interacted strongly with FXII in plasma compared with the glass surface. We also conducted the in situ detection of FXII adsorption onto glass microspheres, both with and without the SPI coating, using the flow-cytometry-based technique[35]. The results aligned with those of the proteomics analysis, showing that the SPI coating adsorbed more FXII (Fig. 5d and Supplementary Figs. 36 and 37). Detailed results and explanation are provided in the Supplementary Results.

Taken together, the results of protein corona analyses and flow-cytometry-based assay allowed us to conclude that the SPI coating exhibits strong interactions with FXII. These results also point to the fact that the strong interaction of FXII with the surface may not be a sufficient condition for the initiation of surface-induced coagulation activation.

Mechanism of modulation of the contact activation by SPI coating

Our data demonstrated that a strong interaction between a surface and FXII may not be a prerequisite condition for its activation and initiation of the contact pathway of coagulation. We further analysed the effect of different surfaces, including the SPI coating (low thrombogenic), HPG/PEG coating (neutral antifouling surface, moderately thrombogenic) and glass (highly thrombogenic), on the contact activation system to probe the mechanism of inhibition of surface-induced thrombogenesis by the SPI coating. Since contact activation in plasma is regulated by various proteins, an in vitro simulation of FXII–PK reciprocal activation was measured in a simplified system (detailed results and explanation are available in the Supplementary Results)[36].

After incubating the FXII–PK mixture with different surfaces, cleavage of the substrate S-2302 was quantified. The catalytic activity of glass and HPG/PEG coating was at least 30 and 4 times higher than that of the SPI coating, respectively (Fig. 6a). The extent of S-2302 cleavage by the different surfaces corresponded with their propensity towards thrombogenesis. This was further confirmed by sodium dodecyl sulfate–polyacrylamide gel electrophoresis (SDS–PAGE) analyses (Supplementary Fig. 38). In the presence of C1INH[37], the catalytic activity of the FXII–PK mixture incubated with the SPI coating was negligible compared with that observed with the glass surface and HPG/PEG coating (Fig. 6b). We observed that these material surfaces did not induce the hydrolysis of FXII and PK in the solution (Supplementary Fig. 39a,b). However, the FXII incubated with the glass surface could significantly enhance the reciprocal activation with PK even after the surface was removed from the solution (Fig. 6c and Supplementary Fig. 41). Unlike the glass surface, such activity was not seen in the case of the SPI coating. Additionally, after incubation with different surfaces, no significant activity changes were observed for FXIIa (Fig. 6d), PK (Supplementary Fig. 39c) and KK (Supplementary Fig. 40), indicating that the inhibition of contact activation by the SPI coating was not due to any changes to FXIIa, PK and KK.

Since the dissociation of FXII after its interaction with different surfaces was detected using flow cytometry (Supplementary Fig. 42), we investigated whether the surface-dissociated FXII undergoes conformational changes. A modified targeted proteomics approach and dimethyl-labelling techniques were applied (Fig. 6e)[38,39]. Our studies revealed that the labelling efficiency of lysine for the surface-dissociated FXII was significantly different from its native state (Fig. 6f), both for the bare glass and SPI-coated surface. However, these structural changes for SPI coating, unlike other surfaces, did not result in the enhanced activity of FXII[36,40] (refer to the detailed explanation in the Supplementary Results). Our hypothesis is summarized in Fig. 6g. For conventional synthetic surfaces, FXII can undergo certain

Fig. 6 | Mechanism of contact activation modulation by SPI coating. **a**, Cleavage efficiency of S-2302 in the absence of inhibitor (C1INH) by an in vitro simulated contact initiation system (400 nM FXII and 400 nM PK in a PBS buffer) after incubation with different surfaces at different time intervals. The slope can represent the catalytic activity of the incubated contact initiation system. $n = 3$ biologically independent samples; all values are expressed as the mean ± s.d. **b**, Cleavage efficiency of S-2302 in the presence of inhibitor (1 μM C1INH) by an in vitro simulated contact initiation system (400 nM FXII and 400 nM PK in a PBS buffer) after incubation with different surfaces at different time intervals. $n = 3$ biologically independent samples; all values are expressed as the mean ± s.d. **c**, FXII solution (final concentration, 400 nM) was first incubated with different surfaces for 10 min and then the solution was co-incubated with PK (final concentration, 400 nM) in a new PP tube, and the cleavage efficiency of S-2302 for the mixture was recorded. $n = 3$ biologically independent samples; all values are expressed as the mean ± s.d. **d**, FXIIa solution (final concentration, 50 nM) was first incubated with different surfaces and then the solution was co-incubated with PK (final concentration, 400 nM) in a new PP tube, and the cleavage efficiency of S-2302 for the mixture was recorded. $n = 3$ biologically independent samples; all values are expressed as the mean ± s.d. **e**, Schematic showing the evaluation of material-induced FXII conformational change using the proteomic approach. **f**, Labelling efficiency for selected dimethyl-labelled lysines. $n = 3$ biologically independent samples; all values are expressed as the mean ± s.d. Multiple comparisons were performed using one-way ANOVA. If significance was attained, post hoc multiple comparisons analysis was conducted with a Tukey's test. Exact P values are provided in the corresponding figures; statistical significance was defined as $P < 0.05$. Individual P values represent comparisons with the native FXII. **g**, Schematic of the mechanistic understanding on how an SPI coating prevents surface-induced thrombosis without interfering with haemostasis.

https://doi.org/10.1038/s41563-024-02046-0

conformational changes that can initiate and enhance contact activation, whether the protein is adsorbed or desorbed from the surface. However, in the case of SPI coating, even though a surface-induced conformational change in FXII is unavoidable, contact activation initiation does not occur, which results in the lack of generation of FXIIa, marked reduction in material-surface-induced thrombogenesis and retention of normal haemostasis.

Outlook

Here we have demonstrated a new concept in the design of a universal antithrombotic surface by altering FXII binding to the surface with favourable haemocompatibility, and that the polymeric coating reduces surface-induced thrombogenesis without interfering with normal haemostasis. The SPI coating, with a sheltered positively charged surface, can prevent the reciprocal activation of FXII–PK

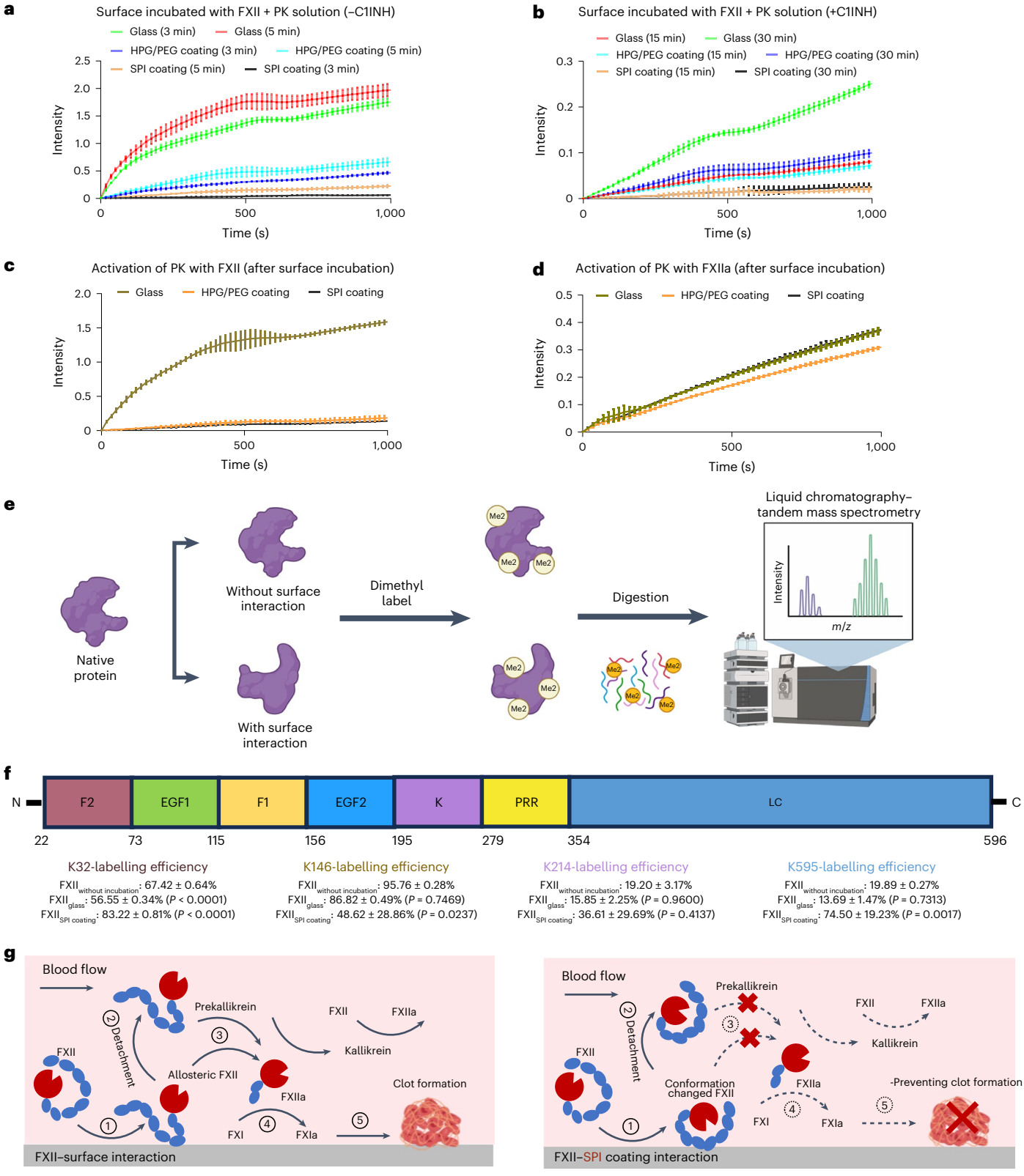

(the 'Supplementary extended outlook' section in the Supplementary Information provides a detailed discussion). Deviating from the conventional wisdom for generating blood-contacting surfaces that utilize protein-resistant or antifouling surfaces, we propose a new direction—by generating a protein-binding SPI coating that avidly interacts with FXII but renders it inactive in terms of initiating the contact pathway of coagulation. We have demonstrated this concept in preventing surface-induced thrombogenesis in both in vitro studies in human blood and using rabbit extracorporeal shunt model without anticoagulant administration.

Besides generating a universal antithrombotic surface for blood-contacting devices, this work also significantly enhances our understanding on the interaction of proteins in the contact pathway with surfaces. This, in turn, provides new design strategies for the next generation of blood-contacting surfaces with improved haemocompatibility. Specifically, we have identified the following. (1) FXII–PK reciprocal activation already occurs under physiological conditions, and antifouling surfaces may increase this activation. Maintaining the activity of the FXII–PK complex affected by surface interaction under physiological conditions is more important in generating an antithrombotic surface. (2) On the basis of our proteomic analyses, coagulation proteins, especially FXII, are adsorbed onto almost all surfaces. However, surface–FXII interaction/binding may not be a prerequisite for the activation of FXII, and all such surface interactions may not increase FXII–PK reciprocal activation. (3) Surface-induced coagulation activation may not be limited to the biointerface. The proteins that are released from the surface can activate coagulation away from the surface. Thus, current strategies used in the development of antithrombotic surfaces that are based on antifouling surfaces (the most commonly used approach) need critical reconsideration. The 'Supplementary extended outlook' section in the Supplementary Information provides an additional discussion.

Although our concept of controlling FXII on the surface led to the generation of a new antithrombotic material, there are still many questions that need to be addressed. The SPI coating attracts more blood proteins than conventional antifouling surfaces. Thus, a key question to be answered is whether single-layer or multilayer adsorption of FXII dominates the SPI coating–FXII interaction. In addition, it is important to understand whether the adsorption of other plasma proteins has a significant impact on the SPI coating–FXII interaction. Is there any correlation between the characteristics of the SPI coating and the specific binding domain of FXII? How does it relate to the desorption behaviour of conformation-altered FXII from the SPI coating? How do different FXII–surface binding sites affect its conformational change[36], which conformations of FXII are prone to induce coagulation activation or inhibition and how stable is the conformation-altered FXII in plasma? These fundamental questions need to be answered in the future and may provide a much deeper understanding on the mechanism(s) of action of the SPI coating and its function as an antithrombotic surface. The current study provides a foundation for such future studies.

Online content

Any methods, additional references, Nature Portfolio reporting summaries, source data, extended data, supplementary information, acknowledgements, peer review information; details of author contributions and competing interests; and statements of data and code availability are available at https://doi.org/10.1038/s41563-024-02046-0.

References

1. Ivanov, I. et al. Proteolytic properties of single-chain factor XII: a mechanism for triggering contact activation. *Blood* **129**, 1527–1537 (2017).
2. Kizhakkedathu, J. N. & Conway, E. M. Biomaterial and cellular implants: foreign surfaces where immunity and coagulation meet. *Blood* **139**, 1987–1998 (2022).
3. Maas, C. & Renne, T. Coagulation factor XII in thrombosis and inflammation. *Blood* **131**, 1903–1909 (2018).
4. Ashcraft, M., Douglass, M., Chen, Y. J. & Handa, H. Combination strategies for antithrombotic biomaterials: an emerging trend towards hemocompatibility. *Biomater. Sci.* **9**, 2413–2423 (2021).
5. Mackman, N. Triggers, targets and treatments for thrombosis. *Nature* **451**, 914–918 (2008).
6. Davenport, A. What are the anticoagulation options for intermittent hemodialysis? *Nat. Rev. Nephrol.* **7**, 499–508 (2011).
7. Mackman, N., Bergmeier, W., Stouffer, G. A. & Weitz, J. I. Therapeutic strategies for thrombosis: new targets and approaches. *Nat. Rev. Drug Discov.* **19**, 333–352 (2020).
8. Jokinen, V., Kankuri, E., Hoshian, S., Franssila, S. & Ras, R. H. A. Superhydrophobic blood-repellent surfaces. *Adv. Mater.* **30**, 1705104 (2018).
9. Maitz, M. F. et al. The blood compatibility challenge. Part 4: surface modification for hemocompatible materials: passive and active approaches to guide blood-material interactions. *Acta Biomater.* **94**, 33–43 (2019).
10. Song, X. et al. Transient blood thinning during extracorporeal blood purification via the inactivation of coagulation factors by hydrogel microspheres. *Nat. Biomed. Eng.* **5**, 1143–1156 (2021).
11. Xu, T. et al. Self-anticoagulant sponge for whole blood auto-transfusion and its mechanism of coagulation factor inactivation. *Nat. Commun.* **14**, 4875 (2023).
12. Fredenburgh, J. C., Gross, P. L. & Weitz, J. I. Emerging anticoagulant strategies. *Blood* **129**, 147–154 (2017).
13. Hedayati, M., Neufeld, M. J., Reynolds, M. M. & Kipper, M. J. The quest for blood-compatible materials: recent advances and future technologies. *Mater. Sci. Eng. R Rep.* **138**, 118–152 (2019).
14. Douglass, M., Garren, M., Devine, R., Mondal, A. & Handa, H. Bio-inspired hemocompatible surface modifications for biomedical applications. *Prog. Mater. Sci.* **130**, 100997–101029 (2022).
15. Smith, R. S. et al. Vascular catheters with a nonleaching poly-sulfobetaine surface modification reduce thrombus formation and microbial attachment. *Sci. Transl. Med.* **4**, 153ra132 (2012).
16. Leslie, D. C. et al. A bioinspired omniphobic surface coating on medical devices prevents thrombosis and biofouling. *Nat. Biotechnol.* **32**, 1134–1140 (2014).
17. Jaffer, I. H., Fredenburgh, J. C., Hirsh, J. & Weitz, J. I. Medical device-induced thrombosis: what causes it and how can we prevent it? *J. Thromb. Haemost.* **13**, S72–S81 (2015).
18. Abbina, S. et al. Blood circulation of soft nanomaterials is governed by dynamic remodeling of protein opsonins at nano-biointerface. *Nat. Commun.* **11**, 3048–3059 (2020).
19. Weber, C., Morsbach, S. & Landfester, K. Possibilities and limitations of different separation techniques for the analysis of the protein corona. *Angew. Chem. Int. Ed.* **58**, 12787–12794 (2019).
20. Vogler, E. A. Protein adsorption in three dimensions. *Biomaterials* **33**, 1201–1237 (2012).
21. Kalathottukaren, M. T. et al. Alteration of blood clotting and lung damage by protamine are avoided using the heparin and polyphosphate inhibitor UHRA. *Blood* **129**, 1368–1379 (2017).
22. Ronco, C. Endotoxin removal: history of a mission. *Blood Purif.* **37**, 5–8 (2014).
23. La, C. C. et al. Smart thrombosis inhibitors without bleeding side effects via charge tunable ligand design. *Nat. Commun.* **14**, 2177–2194 (2023).
24. Shenoi, R. A. et al. Affinity-based design of a synthetic universal reversal agent for heparin anticoagulants. *Sci. Transl. Med.* **6**, 260ra150 (2014).
25. Kalathottukaren, M. T. et al. A polymer therapeutic having universal heparin reversal activity: molecular design and functional mechanism. *Biomacromolecules* **18**, 3343–3358 (2017).

26. Lee, H. A., Ma, Y. F., Zhou, F., Hong, S. & Lee, H. Material-independent surface chemistry beyond polydopamine coating. *Acc. Chem. Res.* **52**, 704–713 (2019).
27. Lundbech, M., Krag, A. E., Christensen, T. D. & Hvas, A. M. Thrombin generation, thrombin-antithrombin complex, and prothrombin fragment F1+2 as biomarkers for hypercoagulability in cancer patients. *Thromb. Res.* **186**, 80–85 (2020).
28. Sperling, C., Maitz, M. F., Grasso, S., Werner, C. & Kanse, S. M. A positively charged surface triggers coagulation activation through factor VII activating protease (FSAP). *ACS Appl. Mater. Interfaces* **9**, 40107–40116 (2017).
29. Frank, R. D. et al. Role of contact system activation in hemodialyzer-induced thrombogenicity. *Kidney Int.* **60**, 1972–1981 (2001).
30. Yang, Z. L. et al. Mussel-inspired catalytic selenocystamine-dopamine coatings for long-term generation of therapeutic gas on cardiovascular stents. *Biomaterials* **178**, 1–10 (2018).
31. Branchford, B. R., Ng, C. J., Neeves, K. B. & Di Paola, J. Microfluidic technology as an emerging clinical tool to evaluate thrombosis and hemostasis. *Thromb. Res.* **136**, 13–19 (2015).
32. Hathcock, J. J. Flow effects on coagulation and thrombosis. *Arterioscler. Thromb. Vasc. Biol.* **26**, 1729–1737 (2006).
33. Mohammad-Beigi, H. et al. Mapping and identification of soft corona proteins at nanoparticles and their impact on cellular association. *Nat. Commun.* **11**, 4535–4550 (2020).
34. Cox, A. et al. Evolution of nanoparticle protein corona across the blood-brain barrier. *ACS Nano* **12**, 7292–7300 (2018).
35. Han, S. et al. Endosomal sorting results in a selective separation of the protein corona from nanoparticles. *Nat. Commun.* **14**, 295–306 (2023).
36. Heestermans, M. et al. Identification of the factor XII contact activation site enables sensitive coagulation diagnostics. *Nat. Commun.* **12**, 5596–5612 (2021).
37. Ivanov, I. et al. A mechanism for hereditary angioedema with normal C1 inhibitor: an inhibitory regulatory role for the factor XII heavy chain. *Blood* **133**, 1152–1163 (2019).
38. Shang, X. Q. et al. Unusual zymogen activation patterns in the protein corona of Ca-zeolites. *Nat. Catal.* **4**, 607–614 (2021).
39. Chen, J. et al. Quantitative lysine reactivity profiling reveals conformational inhibition dynamics and potency of aurora A kinase inhibitors. *Anal. Chem.* **91**, 13222–13229 (2019).
40. Shamanaev, A. et al. Model for surface-dependent factor XII activation: the roles of factor XII heavy chain domains. *Blood Adv.* **6**, 3142–3154 (2022).

[1]Centre for Blood Research & Life Science Institute, University of British Columbia, Life Sciences Centre, Vancouver, British Columbia, Canada. [2]Department of Pathology and Laboratory Medicine, University of British Columbia, Vancouver, British Columbia, Canada. [3]College of Polymer Science and Engineering, State Key Laboratory of Polymer Materials Engineering, Sichuan University, Chengdu, People's Republic of China. [4]School of Biomedical Engineering, University of British Columbia, Vancouver, British Columbia, Canada. [5]Department of Mechanical Engineering, University of British Columbia, Vancouver, British Columbia, Canada. [6]Chengdu First People's Hospital, Chengdu, People's Republic of China. [7]Department of Medicine, University of British Columbia, Vancouver, British Columbia, Canada. ✉e-mail: zhaoscukth@163.com; jay@pathology.ubc.ca

Methods

Ethics statement for blood collection

Our research complies with all the relevant ethical regulations. Human blood was collected at the Centre for Blood Research, University of British Columbia (the protocol for blood collection was approved by the University of British Columbia's clinical ethics board: University of British Columbia Ethics approval nos. H10-01896, H20-00084 and H18-02553) and at the West China Hospital, Sichuan University (GB/T 16886.4-2003/ISO 10993-4:2002, General Administration of Quality Supervision, Inspection and Quarantine of the People's Republic of China, Standardization Administration of the People's Republic of China). Informed written consent was obtained before the blood draw from donors in accordance with the Declaration of Helsinki. Fresh human blood was collected from healthy unmedicated donors using vacutainer blood collection tubes. The use of anticoagulants is described in detail in each experimental section. Blood was centrifuged at 156*g* for 15 min at room temperature to obtain platelet-rich plasma, at 2,000*g* for 15 min to obtain platelet-poor plasma (PPP) or treated by EasySep Direct Human Neutrophil Isolation Kit to obtain neutrophil-rich plasma.

Ethics statement for animal experiments

Our research complies with all relevant ethical regulations. All procedures involving the use of animals in this study were prospectively reviewed and approved by the Institutional Animal Care and Use Committee. This study was conducted in accordance with the National Institutes of Health Guide for the care and use of laboratory animals (NIH publication no. 8023, revised 1978). This experiment conformed to the legal requirement in China and was approved by the ethical committee (no. K2016027) of the West China Hospital, Sichuan University. During the experimental period, the animals had free access to water and food.

Synthesis of modified SPCM

Supplementary Information provides details on the precursors used in the synthesis of SPCM. UHRA-10 (1 g) and 200 mg epoxy-PEG_{400}-azide (~5 mol eq. of UHRA-10) were dried under a vacuum at 60 °C overnight. Then, UHRA-10 was dissolved in 30 ml anhydrous tetrahydrofuran at 70 °C under argon, and 200 mg of NaH was added to the solution. The reaction was kept under stirring at 60 °C for 10 h under argon. After that, 200 mg epoxy-PEG_{400}-azide was dissolved in 20 ml anhydrous tetrahydrofuran, and the solution was added to the reaction solution under argon protection over a period of 10 min under stirring. Then, the reaction was maintained at 75 °C for 24 h. The resulting solution was concentrated by rotary evaporation and was dissolved in 10 ml deionized (DI) water. Then, the product was purified by dialysis (molecular weight cut-off, 2,000) for 24 h, during which the water was changed three times. The solution was dried using a lyophilizer to give the azide-modified UHRA-10. Fourier transform infrared spectra had a peak of 2,100 cm^{-1} (peak of the azido group; Supplementary Fig. 4a). ^1H nuclear magnetic resonance analysis is given in Supplementary Fig. 3b.

After that, 1 g azide-modified UHRA-10 was dried under a vacuum at 60 °C overnight and then dissolved in 80 ml tetrahydrofuran. Then, 400 mg triphenylphosphine was added to the reaction, and after that, 40 ml DI water was added to the solution under stirring for 48 h at 50 °C. After the reaction, the solution was concentrated by rotary evaporation and dissolved in 100 ml DI water, and washed with 100 ml ethyl acetate twice to remove triphenylphosphine and oxidized triphenylphosphine. The resulting water solution was purified by dialysis (molecular weight cut-off, 1,000) for 24 h, during which the water was changed three times. The solution was dried using a lyophilizer to give the final primary-amine-surface-functionalized SPCM. The Fourier transform infrared spectra peak at 2,100 cm^{-1} disappeared.

Synthesis of SPI coating, HPG/PEG coating and PEI coating

The glass substrate was immersed in a dopamine/PEG coating solution (2 mg ml^{-1} dopamine, 10 mg ml^{-1} MeO-PEG-OH (5,000 Da) and 5.3 mg sodium periodate per ml in sodium acetate buffer solution (pH 5)) for 20 min (for glass vials) or 10 min (for glass microspheres). Afterwards, the substrate was washed with DI water to obtain the PDA/PEG coating[41].

For the SPI coating, the PDA/PEG-coated glass was immersed in primary-amine-surface-functionalized SPCM solution (0.5 mg ml^{-1} in phosphate-buffered saline (PBS), pH 8.5) under room temperature for 24 h. For the HPG/PEG coating and PEI coating, the PDA/PEG-coated substrate was immersed in amine–HPG/PEG or PEI (M_n, ~10,000 Da) solution (0.5 mg ml^{-1} in PBS, pH 8.5) under room temperature for 24 h. The HPG/PEG coating and PEI coating were used as control groups for blood analysis. Supplementary Information provides a detailed characterization of the coating.

FXII activation

Citrate-anticoagulated PPP (3.8% sodium citrate with anticoagulant/blood ratio of 1:9) and S-2302 (Chromogenix) were used in this study[1]. To demonstrate the substrate independence of the coating procedure, the coating was applied to glass vials, PS well plate, polypropylene (PP) centrifuge tube, silicone tubing, PVC tubing, polyurethane tubing, titanium cups and glass macroparticle. A mixture of 80 µl of PPP, 20 µl of normal saline and 20 µl of 4 mM substrate S-2302 was incubated with different coatings for 30 min at 37 °C under shaking. Then, 100 µl of the mixture was transferred to a 96-well plate immediately and the optical density (OD) was measured at 405 nm in a plate reader. PPP (80 µl) added with 20 µl normal saline without surface incubation was used as the negative control.

To determine the effect of coatings on FXII activation, different coatings including PDA/PEG, HPG/PEG and SPI were applied on glass vials. The glass vials were incubated with a mixture of 100 µl of PPP, 50 µl of normal saline and 100 µl of 4 mM substrate S-2302 for 30 min at 37 °C under shaking. Then, 100 µl of the mixture was transferred to a 96-well plate immediately and the OD was measured at 405 nm in a plate reader. PPP added with normal saline without surface incubation was used as the negative control. PPP was obtained from at least three individuals, and each experiment was repeated independently at least three times.

BK activation

Activation level of the kallikrein/kinin system by the coating was measured via ELISA (Human BK Enzyme Immunoassay Kit, Abcam)[10]. Different coatings including PDA/PEG, HPG/PEG and SPI were applied to glass vials. Then, 200 µl PPP was introduced and incubated for 30 min at 37 °C under shaking. Finally, the measurements were conducted according to the respective instruction manuals. PPP without incubation was used as the control. PPP was obtained from at least three individuals, and each experiment was repeated independently at least three times.

Thrombin generation

The citrate-anticoagulated PPP and S-2238 (Chromogenix) were used in this study[42]. Different coatings including PDA/PEG, HPG/PEG and SPI were applied to glass vials. Mixture of 80 µl of PPP, 20 µl of 6 mM $CaCl_2$/normal saline (final concentration) and 20 µl of 4 mM substrate S-2238 was incubated with different coatings for 30 min at 37 °C under shaking. After incubation, the reaction was stopped by adding sodium citrate. Thrombin generation was detected by ultraviolet–visible (UV–vis) spectroscopy at 405 nm. PPP was obtained from at least three individuals, and each experiment was repeated independently at least three times.

TAT complex generation

The TAT complex generation was evaluated by ELISA (Human TAT kit, Abcam) method[10]. Different coatings including PDA/PEG, HPG/PEG and SPI were applied to glass vials. Then, 80 µl of citrate-anticoagulated PPP was introduced and the coagulation was triggered by adding 20 µl of

6 mM $CaCl_2$/normal saline (final concentration). The reaction was carried out for 30 min at 37 °C under shaking. After incubation, the reaction was stopped by adding sodium citrate. Then, the plasma samples were collected and the TAT concentration was tested according to the instruction manuals. PPP was obtained from at least three individuals, and each experiment was repeated independently at least three times.

Plasma recalcification times

Different coatings including PDA/PEG, HPG/PEG and SPI were applied on glass vials and PS well plates. Then, 80 µl of citrate-anticoagulated PPP was introduced to each sample and the coagulation was triggered by adding 20 µl of 6 mM $CaCl_2$/normal saline (final concentration). The reaction was carried out at 37 °C under shaking conditions[10]. Clotting times for each sample were recorded. If no thrombus formation was observed after 30 min, the experiment was terminated and the time of experiment was recorded.

For the PPP-clotting time under shear conditions, a closed loop was developed with silicone tubing (Tygon 3350 Sanitary Silicone Tubing) that is approximately 10 cm in length and an inner diameter of 2.4 mm. The closed loop was formed using a straight connector. The uncoated or SPI-coated tubing loop was placed in a peristaltic roller pump (WF300-TH16, PreFluid), and a PBS buffer was circulated through the loop for 10 min. Citrate-anticoagulated PPP (recalcified with 6 mM $CaCl_2$, final concentration) was carefully introduced into the tubing and ensured that no air is introduced (this step is very important as air bubbles can cause severe contact activation). The loop was modelled to simulate flow in the carotid vein; the shear rate of the plasma was 60 s^{-1}. The time of thrombus formation during the experiment was recorded (under 37 °C). If no thrombus formation was observed after 60 min, the experiment was terminated and the time of experiment was recorded. PPP was obtained from at least three individuals, and each experiment was repeated independently at least three times.

aPTT, PT, TT and fibrinogen concentrations

A semiautomatic blood coagulation analyser (CA-50, Sysmex) was used to investigate the influence of SPI coating on the blood coagulation system[10]. Here 300 µl of fresh citrate-anticoagulated PPP was introduced into bare or SPI-coated glass vial and incubated at 37 °C for 30 min. For the aPTT test, 50 µl of the incubated PPP was moved to a test cup and mixed with 50 µl of the aPTT reagent (Dade Actin Activated Cephaloplastin Reagent, Siemens; incubated for 10 min at 37 °C before use). After incubating at 37 °C for 3 min, 50 µl of 25 mM $CaCl_2$ solution was added, and then the aPTT was measured. For the TT test, 50 µl of the incubated PPP was added in a test cup and mixed with 100 µl of the TT reagent (Test Thrombin Reagent, Siemens; incubated for 10 min at 37 °C before use), and then the TT was measured. For the PT test, 50 µl of the incubated PPP was added in a test cup, followed by the addition of 100 µl PT reagent (Thromborel S, Siemens; incubated for 10 min before use), and then the PT was measured. For the detection of the concentration of fibrinogen in plasma, 10 µl of the incubated PPP was added in a test cup and diluted with 50 µl buffer. After incubating at 37 °C for 3 min, the complex solution was mixed with 50 µl thrombin reagent (Sysmex; incubated for 10 min at 37 °C before use), and then the fibrinogen was measured. For all the experiments, at least three parallel samples were applied to get a reliable value, and results were expressed as the mean ± s.d. (n = 3).

Proteomic analysis of SPI-coating-incubated PPP

Fresh citrate-anticoagulated PPP (300 µl) was introduced into bare or SPI-coated glass vial. After incubating for 30 min, the plasma was collected. The sample was grinded with liquid nitrogen into a powder and then transferred to a 5 ml centrifuge tube. After that, four volumes of lysis buffer (8 M urea, 1% protease inhibitor cocktail) were added to the plasma powder, followed by sonication three times on ice using a high-intensity ultrasonic processor (Scientz). The cellular debris from the plasma sample was removed by centrifugation at 12,000g at 4 °C for 10 min. Then, the supernatant was transferred to a new centrifuge tube. The top-14 high-abundance proteins were removed by Pierce Top 14 Abundant Protein Depletion Spin Columns Kit (Thermo Fisher Scientific). Finally, the protein concentration was determined with a bicinchoninic acid kit according to the manufacturer's instructions. Detailed analysis of protein digestion, mass spectrometry analysis and protein identification are given in the 'Extended methods' section in the Supplementary Information.

Detection of the activities of coagulation factors in PPP

An automatic coagulation analyser (ACL Elite Pro, Werfen) was used to investigate the activities of coagulation factors after incubating recalcified PPP with a bare or SPI-coated glass vial. Fresh recalcified PPP (300 µl) was introduced into vials and incubated at 37 °C, and the reaction was stopped by adding sodium citrate after 30 min incubation[10]. For the detection of the activities of FVIII, FIX, FXI and FXII in plasma, 5 µl of the incubated PPP was added in a test cup and diluted with a 45 µl buffer solution. After incubating at 37 °C for 30 s, the complex solution was mixed with 50 µl of the corresponding factor-deficient plasma (coagulation FVIII-deficient plasma, coagulation FIX-deficient plasma, coagulation FXI-deficient plasma and FXII-deficient plasma; Sysmex; incubated for 10 min at 37 °C before use). After another 30 s incubation at 37 °C, 50 µl of the aPTT reagent was added and incubated at 37 °C for 3 min, followed by adding 50 µl of 25 mM $CaCl_2$ solution, and then the factor activity was measured. For all the experiments, at least three parallel samples were measured to get a reliable value, and results were expressed as the mean ± s.d. (n = 3).

Animal model

Thrombogenicity of the medical-grade PVC catheters before and after functionalization by an SPI coating were assessed using an ex vivo AV shunt model in the rabbit[43]. This study was conducted on at least four healthy male New Zealand rabbits aged approximately 4 months old and weighing about 2.5–3.5 kg (without sex preference). The rabbit was anaesthetized with 3% sodium pentobarbital (1 ml kg^{-1}) through an injector placed in an ear vein. The rabbit left carotid artery and the right external jugular vein were isolated through a midline neck incision. Two indwelling needles (22G) were stabbed into the carotid artery and jugular vein, and the blood flow was temporarily blocked by the cover that was supplied with the indwelling needle. Then, bare or SPI-coated catheters were connected with two indwelling needles and the AV custom-built extracorporeal circulation was initiated. Animals had no systemic anticoagulation throughout the experiment. After 30 min, the extracorporeal circulation was terminated, and the blood flow rate through the catheters was checked every 10 min. The blood flow rate was calculated from the volume of outflow within preset time (15 s). After the experiment, the catheter was gently rinsed by normal saline and then all the liquid was pumped out by using a peristaltic pump (BT100 + YZ1515). The residual thrombus in the catheter was collected and weighted. The catheters before and after the treatment were fixed using freshly prepared glutaraldehyde (2.5 wt% in PBS) overnight. The samples were washed with a PBS solution, and subjected to a drying process by passing them through a series of graded alcohol–PBS solutions. Fixed samples were imaged using a field-emission scanning electron microscope (JSM-7500F, JEOL).

The clotting-time assays of the rabbits before and after the experiment were explored by an automatic blood coagulation analyser (CA-7000, Sysmex). For exploring the coagulation activation of the blood after the experiments, blood from the catheter before and after the experiment was dropped into a PS 96-well plate. The whole-blood-clotting time of the blood sample was recorded. It is worth noting that the test methods based on thrombin and fibrinolytic systems to assess coagulation activation are not applicable here, because although the blood from the catheter could still flow and be

collected, the coagulation pathway might be already activated and cannot be inhibited by anticoagulants. At least four parallel sample groups were applied to get a reliable value, and results were expressed as the mean ± s.d.

Proteomic analysis of tightly and loosely bound proteins

As both loosely bound and tightly bound proteins on the surface should have the potential to contribute to the antithrombotic function of the surface, the protein adsorption characteristics on the surface in plasma were explored using proteomics techniques. The loosely and tightly bound proteins on bare or SPI-coated glass vials were in situ digested by trypsin and analysed by liquid chromatography–tandem mass spectrometry; detailed methods are described in the 'Proteomic analysis of SPI coating incubated PPP' section[10] in the Supplementary Information.

Influence of SPI coating on FXII–PK reciprocal activation

The in vitro simulated contact initiation system contains 400 nM FXII and 400 nM PK (from Enzyme Research Laboratories) in a PBS buffer was incubated with glass vials before and after HPG/PEG and SPI modification for different intervals (3 min and 5 min). After the reciprocal activation of FXII and PK, 10 µl of the mixture was transferred to 90 µl of S-2302 substrate solution (2 mM in a PBS buffer) and p-nitroanilide (pNA) generation was detected by UV–vis spectroscopy at 405 nm in a kinetic model and at least three parallel sample groups were applied to get a reliable value. Reducing SDS–PAGE (12% acrylamide) was used to detect the products.

For further exploring the influence of SPI coating–FXII interaction on the contact system under the simulated plasma condition, C1INH (Sigma), a protease inhibitor widely present in blood, was introduced. Contact initiation system contains 400 nM FXII, 400 nM PK and 1 µM C1INH in a PBS buffer and was incubated with uncoated, HPG/PEG-coated and SPI-coated glass vials for different intervals (15 min and 30 min). After the reciprocal activation of PK and FXII, 10 µl of the mixture was transferred to 90 µl of S-2302 substrate solution (2 mM in a PBS buffer) and pNA generation was detected by UV–vis spectroscopy at 405 nm in the kinetic mode.

For exploring whether surface–FXII interaction can result in the activation of FXII, 400 nM FXII was first incubated with glass vials with and without HPG/PEG and SPI coatings for 10 min, and then the solution was transferred to a new PP tube and PK (final concentration, 400 nM) was added and co-incubated for 5 min. Thereafter, 10 µl of the mixture was transferred to 90 µl of S-2302 substrate solution (2 mM in a PBS buffer) and pNA generation was detected by UV–vis spectroscopy at 405 nm in the kinetic mode. At least three parallel sample groups were applied to get a reliable value. Reducing SDS–PAGE (12% acrylamide) was used to detect the products.

For exploring the surface–PK interaction on the function of PK, 400 nM PK was first incubated with uncoated, HPG/PEG-coated and SPI-coated glass vials for 10 min, and then the solution was transferred to a new PP tube and FXII (400 nM, final concentration) was added and co-incubated for 5 min. Thereafter, 10 µl of the mixture was transferred to 90 µl of S-2302 substrate solution (2 mM in a PBS buffer) and pNA generation was detected by UV–vis spectroscopy at 405 nm in the kinetic mode. At least three parallel sample groups were applied to get a reliable value. Reducing SDS–PAGE (12% acrylamide) was used to detect the products.

Active dimethyl labelling and conformation analysis of FXII in plasma by mass spectrometry

Here 1 mg of SPI-coated or uncoated glass microspheres was incubated with 100 µl FXII solution (10 µg/100 µl of a PBS buffer) for 30 min under 37 °C. The FXII solution without surface incubation was used as a blank control. Then, 3.2 µl $NaBH_3CN$ (0.15 M) and 3.2 µl CH_2O (1%) were added, and the reaction was carried out at 37 °C for 20 min. To stop the reaction, 4 µl NH_4HCO_3 (2.5 M) was added and incubated for 20 min. The mixture was centrifuged and the supernatant was collected. Subsequently, the labelled FXII protein present in the supernatant was subjected to chymotrypsin digestion following the instructions provided with the reagents (https://assets.fishersci.com/TFS-Assets/LSG/manuals/MAN0011638_Mass_SpectroGrade_Endoprotein_UG.pdf). Detailed information on mass spectrometry analysis and protein identification are given in the 'Extended methods' section in the Supplementary Information.

Statistical analysis. Most experiments were repeated for a minimum of three independent analyses unless mentioned otherwise. In general, data are expressed as the mean ± s.d. Statistical analysis was performed using GraphPad Prism 8. A difference with a P value of less than 0.05 was considered statistically significant. Data distribution was assumed to be normal but this was not formally tested. Data were statistically analysed with unpaired, two-tailed Student's t-test (Figs. 2a and 4c and Supplementary Figs. 16, 20, 24 and 27); paired, two-tailed Student's t-test (Fig. 4d,f); unpaired, one-way analysis of variance (ANOVA) followed by Tukey's post hoc tests (Figs. 2b–e and 3a,f,g and Supplementary Figs. 12, 14, 15, 17–19, 21–23, 25, 28–30, 34 and 36); and paired, one-way ANOVA (Fig. 4b). In substrate course analyses, a mixed two-way ANOVA with Bonferroni's post hoc tests were used (Fig. 2a). No statistical methods were used to predetermine the sample sizes, but our sample sizes are similar to those reported in previous publications[10,11,23,38,44]. For Figs. 1–3, 5 and 6 and the associated supplementary figures, data collection and analysis were not performed blind to the conditions of the experiments. For Fig. 4 and the associated supplementary figures, rabbits were randomly assigned to experimental groups, and operators were blinded to the group assignments. No animals or data points were excluded from the analyses. All results were consistent across independent experiments. The findings in this study were replicated independently with different groups, and the data collection was randomized.

Reporting summary

Further information on research design is available in the Nature Portfolio Reporting Summary linked to this article.

Data availability

Protein mass spectra were searched against the human SwissProt database (20,422 entries) concatenated with the reverse decoy database (proteome ID: UP000005640; release nos. 2021_01/2021_01). Proteomic data, including raw data and search results, have been deposited in the ProteomeXchange database with dataset identifier PXD054476 (for Figs. 3b and 5b,c) and PXD054293 (for Fig. 6f). All other data supporting the findings of this study are available within the Article and its Supplementary Information and available from the corresponding authors on request. Source data are provided with this paper.

References

41. Ryu, J. H., Messersmith, P. B. & Lee, H. Polydopamine surface chemistry: a decade of discovery. *ACS Appl. Mater. Interfaces* **10**, 7523–7540 (2018).
42. Smeets, R. et al. A novel hemostatic delivery device for thrombin: biodegradable poly(D,L-lactide-*co*-glycolide) 50:50 microspheres. *J. Biomed. Mater. Res.* **96A**, 177–185 (2011).
43. Qiu, H. et al. Phenolic-amine chemistry mediated synergistic modification with polyphenols and thrombin inhibitor for combating the thrombosis and inflammation of cardiovascular stents. *Biomaterials* **269**, 120626 (2021).
44. Ivanov, I. et al. Protease activity in single-chain prekallikrein. *Blood* **135**, 558–567 (2020).

Acknowledgements

We thank the Center for Blood Research (CBR) for the use of their research facilities and access to the University of British Columbia

bioimaging facility. We acknowledge funding from the Canadian Institutes of Health Research (CIHR) to J.N.K., and the Natural Sciences and Engineering Council of Canada (NSERC; to J.N.K. and E.M.C.). The infrastructure facility is supported by the Canada Foundation for Innovation (CFI) and the British Columbia Knowledge Development Fund (BCKDF). W.Z. and C.Z. acknowledge funding from the National Natural Science Foundation of China (nos. 52073190 and 52122306). J.N.K. is a Tier 1 Canada Research Chair in Immunomodulating Materials and Immunotherapy. H.J. acknowledges financial support from the China Scholarship Council (CSC) to study as a visiting student at the University of British Columbia and a Postdoctoral Research Trainee award from Michael Smith Health Research BC, and motivation from L. Xiong. We thank PTM BIO (Hangzhou, China) for providing blood and data-independent acquisition for the quantitative proteome analysis, and the research group of L. Foster (University of British Columbia) and J. Rogalski for help with the targeted proteomic experiments.

Author contributions

H.J. provided the early conception of SPI coating–FXII interaction to prevent surface-induced contact activation and designed the experiments. J.N.K. conceived and provided the conceptual revision, technical advice and supervision. H.J., S.A. and I.C. designed and conducted the chemical synthesis. H.J. and K.Y. designed and conducted the coating development and characterization. H.J. designed and conducted the blood tests and haemocompatibility characterization. M.M.R. assisted in performing the cytotoxicity and cell adhesion experiments with H.J. K.Y. and M.D. provided help for the platelet and neutrophil adhesion and activation tests. S.V. provided help for the tests using laser confocal microscopy. L.X., Y.L., T.X. and S.C. designed and conducted the animal experiments. S.M.A.A. and D.G. designed and conducted the blood flow simulation. T.X. and S.C. provided help for the proteomics. K.G. and E.M.C. provided help with the protein characterization and complement activation analyses. H.J. and J.N.K. drafted the manuscript. J.N.K., E.M.C., C.Z. and W.Z. revised the manuscript. J.N.K., C.Z. and W.Z. supervised the study and provided funding for the study. All authors gave approval for the final version of the manuscript.

Competing interests

All authors declare no competing interests.

Additional information

Supplementary information The online version contains supplementary material available at https://doi.org/10.1038/s41563-024-02046-0.

Correspondence and requests for materials should be addressed to Weifeng Zhao or Jayachandran N. Kizhakkedathu.

Peer review information *Nature Materials* thanks Ashutosh Chilkoti, Manfred Maitz and the other, anonymous, reviewer(s) for their contribution to the peer review of this work.

nature portfolio

Corresponding author(s): Weifeng Zhao, Jayachandran N Kizhakkedathu

Last updated by author(s): Oct 1, 2024

Reporting Summary

Nature Portfolio wishes to improve the reproducibility of the work that we publish. This form provides structure for consistency and transparency in reporting. For further information on Nature Portfolio policies, see our Editorial Policies and the Editorial Policy Checklist.

Statistics

For all statistical analyses, confirm that the following items are present in the figure legend, table legend, main text, or Methods section.

n/a	Confirmed	
☐	☒	The exact sample size (*n*) for each experimental group/condition, given as a discrete number and unit of measurement
☐	☒	A statement on whether measurements were taken from distinct samples or whether the same sample was measured repeatedly
☐	☒	The statistical test(s) used AND whether they are one- or two-sided *Only common tests should be described solely by name; describe more complex techniques in the Methods section.*
☐	☒	A description of all covariates tested
☐	☒	A description of any assumptions or corrections, such as tests of normality and adjustment for multiple comparisons
☐	☒	A full description of the statistical parameters including central tendency (e.g. means) or other basic estimates (e.g. regression coefficient) AND variation (e.g. standard deviation) or associated estimates of uncertainty (e.g. confidence intervals)
☐	☒	For null hypothesis testing, the test statistic (e.g. *F*, *t*, *r*) with confidence intervals, effect sizes, degrees of freedom and *P* value noted *Give P values as exact values whenever suitable.*
☒	☐	For Bayesian analysis, information on the choice of priors and Markov chain Monte Carlo settings
☒	☐	For hierarchical and complex designs, identification of the appropriate level for tests and full reporting of outcomes
☒	☐	Estimates of effect sizes (e.g. Cohen's *d*, Pearson's *r*), indicating how they were calculated

Our web collection on statistics for biologists contains articles on many of the points above.

Software and code

Policy information about availability of computer code

Data collection

Bruker Avance AV-300 spectrometer was used to acquire NMR spectra of designed moleculars.
Bruker 670 TensorII with an MCT/A liquid nitrogen cooled detector was used to collect FTIR spectra of designed moleculars and coatings.
Leybold LH Max 200 surface analysis system (Leybold, Cologne, Germany) equipped with a Mg Kα source at a power of 200 W was used to collect XPS spectra of designed coatings.
QCM-D (Biolin Scientific) was used for evaluation of the mass and stability of the coating on the sensor surface.
The coating thickness was obtained from ellipsometer (M-2000V, J.A. Woollam Co., Inc.).
The surface-morphologies were obtained by scanning electron microscopy (SEM, Phenom Pure, Phenom World, Netherlands).
The image of the water droplets on the surfaces were taken with a digital camera (Retiga 1300, Q-imaging Co.).
The surface zeta potentials of the coated substrates were measured using a Zetasizer Nano-ZS90 (Malvern Instruments Ltd., UK).
Blood clotting, pNA generation, and chromogenic substrate based results was detected by UV-VIS at 405 nm in kinetic mode.
A semiautomatic blood coagulation analyzer (CA-50, Sysmex Corporation, Japan) was employed to investigate the influence of SPI coating on the blood coagulation system.
The peptides were subjected to capillary source followed by the timsTOF Pro (Bruker Daltonics) mass spectrometry.
An automatic coagulation analyzer (ACL Elite Pro, werfan) was employed to investigate the activities of coagulation factors after incubating recalcified PPP with bare or SPI-coated glass vial.
3-Laser CytoFLEX Flow Cytometer (Beckman Coulter Life Sciences, Indianapolis, IN, USA) was used for flow cytometry.
The whole blood cell differential counts were measured by an automated hematology cell analyzer (BC-5100, Mindray Bio-Medical Electronics Co., Ltd., Shenzhen, China).
Blood flow simulation using computational fluid dynamics (CFD) modewas was carried out in COMSOL Multiphysics, and an extra fine mesh was generated for the computational domain.

Data analysis	Microsoft Excel 2019, OriginPro 2018, Prism Graphpad 7.0, imageJ 1.53t, OMNIC 8, Avantage 5.967, BD FACSCanto II, Q-Sense Dfind, Northern Eclipse software were used. Mass spectra were searched against the human SwissProt database (20422 entries) concatenated with reverse decoy database using MaxQuant 1.6.15.0.

For manuscripts utilizing custom algorithms or software that are central to the research but not yet described in published literature, software must be made available to editors and reviewers. We strongly encourage code deposition in a community repository (e.g. GitHub). See the Nature Portfolio guidelines for submitting code & software for further information.

Data

Policy information about availability of data

All manuscripts must include a data availability statement. This statement should provide the following information, where applicable:

- Accession codes, unique identifiers, or web links for publicly available datasets
- A description of any restrictions on data availability
- For clinical datasets or third party data, please ensure that the statement adheres to our policy

Protein mass spectra were searched against the human SwissProt database (20422 entries) concatenated with reverse decoy database; proteome ID: UP000005640; release numbers: 2021_01/2021_01). Proteomic data, including raw data and search results have been deposited in the ProteomeXchange database with dataset identifier "PXD054476 (for Fig. 3b and 5b-c) and PXD054293 (for Fig. 6f)". All other data supporting the findings of this study are available within the article and its supplementary files.

Human research participants

Policy information about studies involving human research participants and Sex and Gender in Research.

Reporting on sex and gender	All blood samples were collected from healthy donors, and gender differences were not considered.
Population characteristics	Fresh human blood was collected from healthy, unmedicated donors aged 20-30 using vacutainer blood collection tubes, with no gender preference.
Recruitment	University of British Columbia and the West China Hospital announced the recruitment of human research participants. These volunteers were recruited by voluntary registration and disease-history screening. Volunteers with no recent use of medications affecting the coagulation system and no history of coagulation disorders were selected, as these factors could influence the experimental results regarding the material's interaction with the coagulation system.
Ethics oversight	University of British Columbia (the protocol for blood donations was approved by the University of British Columbia's clinical ethics board. UBC Ethics approval no: H10-01896, H20-00084 and H18-02553) and West China Hospital, Sichuan University (GB/T 16886.4-2003/ISO 10993-4:2002, General Administration of Quality Supervision, Inspection and Quarantine of the People's Republic of China, Standardization Administration of the People's Republic of China).

Note that full information on the approval of the study protocol must also be provided in the manuscript.

Field-specific reporting

Please select the one below that is the best fit for your research. If you are not sure, read the appropriate sections before making your selection.

☒ Life sciences ☐ Behavioural & social sciences ☐ Ecological, evolutionary & environmental sciences

For a reference copy of the document with all sections, see nature.com/documents/nr-reporting-summary-flat.pdf

Life sciences study design

All studies must disclose on these points even when the disclosure is negative.

Sample size	For animal experiments, we analyzed samples with a minimum of 4 rabbits to determine statistical similarity or differences between groups. No statistical methods were used to pre-determine the sample size. Our sample sizes are similar to those reported in previous publications: Qiu H, Tu QF, Gao P, Li XY, Maitz MF, Xiong KQ, et al. Phenolic-amine chemistry mediated synergistic modification with polyphenols and thrombin inhibitor for combating the thrombosis and inflammation of cardiovascular stents. Biomaterials, 269 (2021) 120626 Leslie DC, Waterhouse A, Berthet JB, Valentin TM, Watters AL, Jain A, et al. A bioinspired omniphobic surface coating on medical devices prevents thrombosis and biofouling. Nat Biotechnol 2014, 32(11): 1134-1140
Data exclusions	No data acquired for quantitative analysis was excluded from the study.

Replication	Unless otherwise mentioned, at least 4 replications were performed for all the tests. All our attempts at replication were successful with similar results.
Randomization	All New Zealand rabbits were randomly assigned to experimental groups for all experiments.
Blinding	The establishment of animal experimental models and data collection were conducted by the same team, which was blinded to the sample groups. Samples from different groups were randomly assigned to operators for experimentation. During the subsequent blood tests, these samples were pooled and numbered in a manner that did not reveal their group characteristics. The analysis involving blood coagulation parameters, SEM, blood count assay, computational fluid dynamics (CFD) model, biological parameters were not blinded as the results comes from computational and mathematical analysis which is not effected by individual interpretation.

Reporting for specific materials, systems and methods

We require information from authors about some types of materials, experimental systems and methods used in many studies. Here, indicate whether each material, system or method listed is relevant to your study. If you are not sure if a list item applies to your research, read the appropriate section before selecting a response.

Materials & experimental systems

n/a	Involved in the study
☐	☒ Antibodies
☐	☒ Eukaryotic cell lines
☒	☐ Palaeontology and archaeology
☐	☒ Animals and other organisms
☒	☐ Clinical data
☒	☐ Dual use research of concern

Methods

n/a	Involved in the study
☒	☐ ChIP-seq
☐	☒ Flow cytometry
☒	☐ MRI-based neuroimaging

Antibodies

Antibodies used	Anti-CD42-fluorescein isothiocyanate (FITC, BD, biosciences, 555473); anti-CD62P-phycoerythrin (PE, BD, biosciences, 550561); allophycocyanin (APC) anti-human CD15 (Biolegend, 301908); FITC anti-human CD11b (Biolegend, 301330) for flow cytometry and laser scanning confocal microscope measurements. Antibodies for Human Bradykinin (BK) (Abcam, USA, ab136936), Thrombin-antithrombin (TAT) complex (Human TAT kit, Abcam, USA, ab108907), IL-6 (Thermo Fisher, 88-7066-22), FVIIa level (Human Factor VIIa Chromogenic Activity Assay Kit, ab137995), C3a and C5b-9 generation (Complement C3a Human ELISA Kit, Fisher scientific, 50-112-5293; Complement C5b-9 Human ELISA Kit, Quidel, San Diego, CA, A020(QI)) and FDP level (FDP ELISA Kit, Abbexa Ltd., ABX151504-96TESTS) were provided by the respective vendors along with their kits.
Validation	Validation of Flow cytometry of human platelets for Anti-CD42-fluorescein isothiocyanate (FITC, BD, biosciences, 555473) and anti-CD62P-phycoerythrin (PE, BD, biosciences, 550561) can be found in:https://www.bdbiosciences.com/content/dam/bdb/products/global/reagents/flow-cytometry-reagents/research-reagents/single-color-antibodies-ruo/555xxx/5554xx/555472_base/pdf/555472.pdf, and https://www.bdbiosciences.com/content/bdb/paths/generate-tds-document.cn.550561.pdf#:~:text=Anti-Human%20CD62P%20(Cat.%20No.%20550561;%20solid. Validation of Flow cytometry of human neutrophils for forallophycocyanin (APC) anti-human CD15 (Biolegend, 301908); FITC anti-human CD11b (Biolegend, 301330) can be found in: https://d1spbj2x7qk4bg.cloudfront.net/en-gb/products/apc-anti-human-cd15-ssea-1-antibody-3702?displayInline=true&filename=APC%20anti-human%20CD15%20(SSEA-1)%20Antibody.pdf&leftRightMargin=15&pdf=true&topBottomMargin=15&v=20240910063028, and https://d1spbj2x7qk4bg.cloudfront.net/en-gb/products/fitc-anti-human-cd11b-antibody-8299?displayInline=true&filename=FITC%20anti-human%20CD11b%20Antibody.pdf&leftRightMargin=15&pdf=true&topBottomMargin=15&v=20240814063131. Validation of Elisa test of human BK (Abcam, USA, ab136936) and TAT (Human TAT kit, Abcam, USA, ab108907) can be found in: https://www.abcam.com/en-us/products/elisa-kits/bradykinin-elisa-kit-ab136936, and https://www.abcam.com/en-us/products/elisa-kits/human-thrombin-antithrombin-complex-elisa-kit-tat-ab108907. Validation of Elisa test of human IL-6 (Thermo Fisher, 88-7066-22), FVIIa level (Human Factor VIIa Chromogenic Activity Assay Kit, ab137995), C3a and C5b-9 generation (Complement C3a Human ELISA Kit, Fisher scientific, 50-112-5293; Complement C5b-9 Human ELISA Kit, Quidel, San Diego, CA, A020(QI)) and FDP level (FDP ELISA Kit, Abbexa Ltd., ABX151504-96TESTS) can be found in: https://www.thermofisher.com/elisa/product/IL-6-Human-Uncoated-ELISA-Kit-with-Plates/88-7066-22#documents-container, https://www.abcam.com/en-ca/search/page?facets.categoryType=Assay%20Kits&productSorting=&resourceSorting=relevance&keywords=factor%20viiia%20assay, https://www.fishersci.com/shop/products/human-c3a-platinum-elisa-kit-4/501125293#:~:text=eBioscience%20Human%20C3a%20Platinum%20ELISA%20Kit:, https://www.quidelortho.com/ca/en/products/microvue-assays/microvue-sc5b-9-plus-eia#1-item-c59d5a7bd7-tab, and https://www.abbexa.com/human-fdp-elisa-kit, respectively.

Eukaryotic cell lines

Policy information about cell lines and Sex and Gender in Research

Cell line source(s)	EA.hy926 cells were purchased from American Type Culture Collection (ATCC, CRL-2922) and used up to a passage number of 50. Human vascular smooth muscle cells (HVSMC, ATCC, PCS-100-012) were used to evaluate the SMC proliferation on SPI coating.

Authentication	The EA. hy926 cells were authenticated at the time of purchase from ATCC. Electron photomicrographs of EA. hy926 cells demonstrate cytoplasmic distribution of Weibel-Palade bodies and tissue-specific organelles, characteristics of differentiated endothelial cell functions such as angiogenesis, homeostasis/thrombosis, blood pressure and inflammation. Cell lines were not authenticated for Human vascular smooth muscle cells.
Mycoplasma contamination	The cell lines were not tested for mycoplasma contamination
Commonly misidentified lines (See ICLAC register)	No cells used in this study are commonly misidentified lines

Animals and other research organisms

Policy information about studies involving animals; ARRIVE guidelines recommended for reporting animal research, and Sex and Gender in Research

Laboratory animals	Healthy New Zealand White Rabbits (aged approximately 4 mouths and weighing about 2.5–3.5 kg, Laboratory Animal Center of West China Hospital Science Park, Sichuan University)
Wild animals	No wild animals were used in this study.
Reporting on sex	Gender differences were not considered
Field-collected samples	No field-collected samples were used in this study
Ethics oversight	This study was conducted in accordance with the National Institutes of Health Guide for the care and use of laboratory animals (NIH Publications No. 8023, revised 1978). This experiment conformed to the legal requirement in China and was approved by the ethical committee (No. K2016027) of West China Hospital, Sichuan University.

Note that full information on the approval of the study protocol must also be provided in the manuscript.

Flow Cytometry

Plots

Confirm that:

☒ The axis labels state the marker and fluorochrome used (e.g. CD4-FITC).

☒ The axis scales are clearly visible. Include numbers along axes only for bottom left plot of group (a 'group' is an analysis of identical markers).

☐ All plots are contour plots with outliers or pseudocolor plots.

☒ A numerical value for number of cells or percentage (with statistics) is provided.

Methodology

Sample preparation	Human platelets and neutrophils were used for analysis, details are given in the supplementary information. For protein corona tests, glass microspheres (Sigma) with a diameter of 3 um were used.
Instrument	BD FACSCanto II flow cytometer
Software	CytExpert 2.5
Cell population abundance	For platelet and neutrophil activation tests, a total of 10,000 events were collected for each samples for platelet and neutrophil activation tests. For protein corona tests, a total of 500,000 events were collected for each samples.
Gating strategy	The CD42-gated platelets were used for platelet activation test;the CD15-gated neutrophils were used for neutrophil activation tests; for the protein corona tests, there is no gating strategy since the significantly higher number of microspheres compared to impurities in the plasma

☒ Tick this box to confirm that a figure exemplifying the gating strategy is provided in the Supplementary Information.